Thermal imaging as a method to study the effect of induced ischemia on vasomotion

Annabel Bantle, Christian Korfitz Mortensen, Toby Steven Waterstone

December 19, 2017

Abstract

Vasomotion is an autoregulatory mechanism that optimizes blood distribution within the microcirculatory system. Thermal imaging is a promising approach to measure this phenomena. Previous studies have detected that vasomotion is quantifiable as temperature micro oscillations in the endothelial (0.005 - 0.02 Hz), neurogenic (0.02 - 0.05 Hz) and myogenic (0.05 - 0.15 Hz) frequency band. Four healthy subjects were recruited to investigate the possibilities of measuring changes in vasomotric activity caused by partial brachial occlusion of blood supply by using thermal imaging. Measurements were done as a baseline and with 50% restriction of hand's blood supply by brachial cuff. Data processing involved correction of artifacts seen in the temperature recordings. Morlet continuous wavelet transform was used on the corrected temperature recording to find the frequency content in the micro temperature oscillations. A paired t-test within the frequency bands showed no significant difference between the mean magnitude values of baseline (endothelial 6.71±1.90, neurogenic 5.05±0.65, myogenic 4.66±0.77) and restriction (endothelial 5.95±0.75, neurogenic 4.82±0.95, myogenic 4.70±0.72). Results show thermal imaging might not be sensitive enough to detect changes in vasomotion during a 50% restriction of blood supply, and clear limitations in the experimental setup.

I. Introduction

The use of thermal imaging to study the phenomena of vasomotion might present a new biomarker for the treatment of patients going into shock.[1,2] Vasomotion is the phenomena of oscillating changes in the capillary vessel diameter enforced by smooth muscle cells. This phenomena occurs in the microcirculatory system as an autoregulatory mechanism that optimizes blood distribution within the microcirculatory system.[3-6] Changes in micro temperature oscillations are the source of thermal waves, from the blood flow, propagating from microvessels toward the skin surface.[7] Although several studies have investigated the occurrences of vasomotion within the capillary network, only few have used thermal imaging as detection method.[8-10] With a better knowledge of vasomotion it might possible to give an earlier prediction, if patients are developing shock. Particularly patients who are in danger of developing hypoxia due to shock, as this affects alterations in the microcirculatory system and interfere with the perfusion.[1,2] New methods for studying vasomotric activity arise and thermal imaging presents advantages in larger sample area and by being non-invasive. Previous studies detected that the vasomotric blood flow is quantifiable as micro temperature oscillations within three frequency bands of endothelial ($0.005 - 0.02\ Hz$), neurogenic ($0.02 - 0.05\ Hz$) and myogenic ($0.05 - 0.15\ Hz$) origin.[3,7-9] The significance of these frequency band during disease are for instance shown in a decrease in amplitude of endothelial blood flow oscillations which assumed to be a biomarker for en-

dothelial dysfunction, that indicates cardiovascular disorders such as arterial hypertension and cardiac ischemia.[7] Therefore the interest of this study was to investigate thermal imaging's ability to detect, if there are changes in the micro temperature oscillations depending on hypoxia in the microcirculatory system.

II. Methodology

i. Subjects

Four healthy subjects, 3 males and 1 female, average age 30.5 ± 12.5 years were recruited. Two subject were right handed and two left handed. No subjects consumed caffeine, alcoholic beverages, or medicine before the experiment. All subjects were aware of the experimental procedure and were willing to participate. Subjects showed no signs of cardiac disease or tremors.

ii. Test setting

Subjects were placed in an upholstered adjustable chair for a comfortable sitting position. The hand was stabilized by a vacuum pillow covered with micro fiber tissue, which was attached on the armrest. Xenics Gobi 640 $17\mu m$ GigE infrared camera (Xenics NV, Belgium),sensitivity 0.05°, resolution 480 x 640, was positioned with a tripod 37.5 ± 1.0 cm over subject's dominant hand and connected via Ethernet cable with a computer (figure 1).

Figure 1: *The experimental setup at Region Hospital Nordjylland.*

iii. Software setting

Xeneth 2.6 software (Xenics NV, Belgium), installed on computer, was used for data acquisition. The sampling rate was set to 6.25 Hz, the file format to a raw data xvi-file and both, room and ambient temperature, to $25°C$ and emissivity of observed object to 1.

iv. Experimental procedure

2 x 20 min data acquisition periods were planned. One as a baseline, and another where blood flow restriction enforces hypoxia[4]. The camera was set to warm up for at least 15 min. Meanwhile systolic blood pressure was measured to determine total occlusion pressure (TOP) of subject's dominant arm. Needed brachial cuff pressure (p_{cuff}) for restricting 50% blood flow is 30% of the TOP. TOP was calculated with $p_{cuff} = TOP \times 0.3$.[11] The subjects had at least 30 min to adjust to the room temperature.
The brachial cuff for enforcing blood flow restriction in the second acquisition period was affixed on the subject's dominant arm without tightening it before both measurements. The subject was placed in the chair and the dominant hand was stabilized with the vacuum pillow. The lens was adjusted, so the hand was in focus.
To minimize any possible movement bias the subject was not allowed to move or speak during the whole procedure.

v. Data processing

v.1 Preparation of data

The acquired xvi-files were read and processed in MATLAB R2017b. The header in the beginning of each file and frame was removed. Afterwards the raw uint 16 pixel intensities were divided into frames.

v.2 Regions of interest

28 regions of interest (ROIs) were selected on behalf of getting full representation of the hand

(figure 2). Each region represented one pixel intensity in the 640 x 480 image matrix.

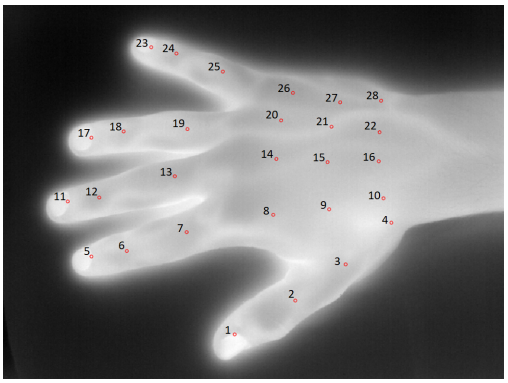

Figure 2: *Frame from thermal image of subject 1. Red dots are indicating the 28 ROIs, with respective numbering.*

This pixel represented an area of the hand with a width of approximately 417μm.

v.3 Artifacts

Under visual inspection of the temperature trace over time, some unexplainable discontinuities were present. These discontinuities were characterized as artifacts made by the camera[12,13]. From the raw data of all regions, three types of artifacts were characterized. A white noise component is observed during the whole recording, intervals between two discontinuities containing a drift component and adjustments by the shutter from non-uniformity correction due to the drift component. All artifacts are shown in figure 3, which is representing one temperature trace from a region.
The artifacts are assumed to occur because each microbolometer in the focal plane array has a different response to the same infrared excitation. This caused the camera to perform non-uniformity corrections, where all microbolometers are re-calibrated, resulting in an offset.[12,13]

v.4 Correction method

The shutter adjustments and the drift between these adjustments, seen in figure 3, corrupted

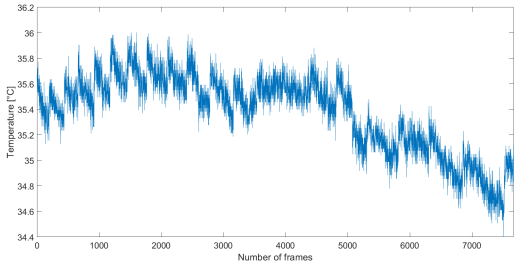

Figure 3: *Raw temperature trace in relation to frame number of region 15 in baseline recording of subject 1, showing outline of the artifacts as discontinuities.*

the raw temperature trace the most. Therefore a correction method based on linear regression was implemented. The linear regression was made on each drift between shutter adjustments. As shown in figure 4, the regression lines were put together at the middle point of an adjustment forming a new temperature recording base. Figure 5 shows how the residuals are projected on to the newly corrected base forming a new temperature trace.

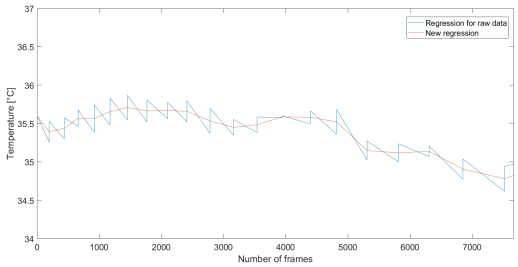

Figure 4: *Connected regression line of raw temperature trace of baseline recording from subject 1 in ROI 15 plotted in blue. New oriented regression line of the same recording plotted in red.*

v.5 Time-frequency analysis

Analysis of the corrected data was done in the time frequency domain by the use of Morlet continues wavelet transform (CWT). The CWT present higher resolution of frequency content in low frequency signals, compared to the Fourier transformation.[7,8]
In the CWT, the signal is convoluted with the

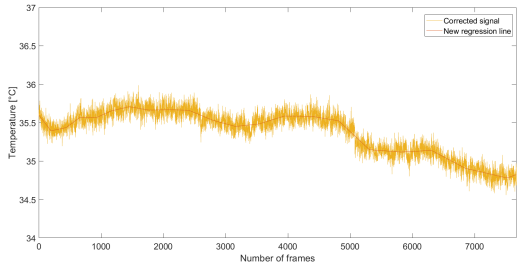

Figure 5: *New oriented regression line based on temperature trace of baseline recording from subject 1 in ROI 15 plottet in red. Corrected temperature trace of the same baseline recording plottet in yellow.*

Morlet wavelet in equation 1:

$$W(\tau, s) = \int_{-\infty}^{\infty} x(t) \frac{1}{\sqrt{\mid s \mid}} \psi * (\frac{t-\tau}{s}) dt \quad (1)$$

Where $x(t)$ is the signal and ψ is the Morlet wavelet. W denotes the wavelet transformation magnitude in relation to the time τ and frequency s. A scalogram showing the time-frequency content of the uncorrected temperature trace given as output of the CWT can be seen in figure 6.

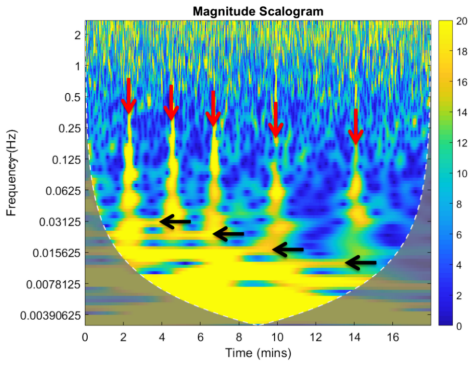

Figure 6: *Scalogram from subject 3 in ROI 8, uncorrected baseline recording. Red arrows showing frequency content of discontinuities in the temperature trace and black arrows showing frequency content of drift artifacts*

The discontinuities within the temperature trace are clearly shown as high magnitude spikes in the scalogram. In figure 6 those spikes are marked with red arrows. The black arrows mark the drift that is contained in between each discontinuity, as seen the drift decrease in frequency.

After application of the correction method, each temperature trace and its corresponding scalogram were submitted a manual control. During this control it was noticed that some temperature traces still contained discontinuities which hampered correct data analysis for those temperature traces. Five RIOs have been chosen valid for further data analysis. The criterion for this selection was, that those ROIs showed good response to the correction method and no discontinuities visible in the scalogram. The five selected ROIs were 10, 14, 20, 21 and 22, those can be seen in figure 2.

The corrected temperature trace from figure 6 is shown in figure 7, which is also illustrating the frequency bands of interest.

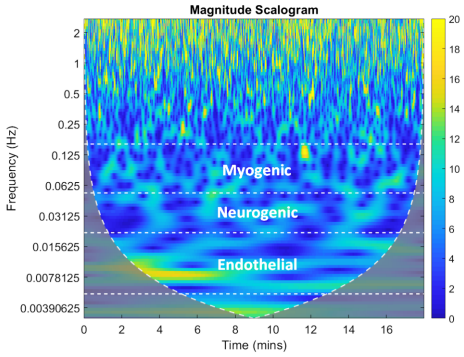

Figure 7: *Scalogram from subject 3 in ROI 8, corrected baseline recording. Frequency bands of endothelial, neurogenic and myogenic are shown.*

The combination of a valid corrected temperature trace across all subjects corresponding to the same ROI is needed for equally comparison between subjects, why only five regions could be used for further data analysis.

vi. Statistical approach

The magnitude within the scalograms of both conditions was compared for each subject. This comparison was conducted for the five ROI within the endothelial, neurogenic and myogenic frequency band. In every recording one

mean magnitude value was calculated for each frequency band.[14] To test the statistical significance of the difference between the mean magnitudes a paired t-test has been applied.

III. Results

The box plots shown in figure 8(appendix) display the mean magnitude of each frequency band for each subject ordered by color in both conditions. The line connecting baseline and restriction condition indicates if the magnitude increased or decreased.

Throughout the combination of frequency band and regions, no clear pattern is visible for the four subjects. In each frequency band the mean magnitude both increase and decrease for each subject. Only subject 2 shows a clear pattern before and after the intervention, where mean magnitude seem to decrease in every frequency band and region.

Table 1 illustrates a mean magnitude value for endothelial, neurogenic and myogenic frequency band in the baseline and restricted measurement. The mean magnitude values are representing all subjects and ROIs.

Table 1: *Table showing the mean magnitudes of each frequency band in both measured conditions.*

	mean endo	**mean neuro**	**mean myo**
Baseline	6.71±1.90	5.05±0.65	4.66±0.77
Restriction	5.95±0.75	4.82±0.95	4.70±0.72

With the values visualized by the box plots in figure 8 a paired t-test provided the following p-values (table 2).

Table 2: *Table showing the p-values corresponding to specific ROI in correlation with frequency band.*

	p-endo	**p-neuro**	**p-myo**
ROI 10	0.71	0.93	0.84
ROI 14	0.62	0.69	0.92
ROI 20	0.41	0.80	0.84
ROI 21	0.40	0.84	0.95
ROI 22	0.38	0.15	0.93

IV. Discussion

This study investigated the hypothesis, if thermal imaging is sensitive enough to measure the effects of vasomotion activity, and thereby investigate if changes in the microcirculatory system caused by a 50 % restriction of blood flow occur.

i. Results

The obvious assumption, based on the presented p-values, that there are no changes in the microcirculatory system or rather in vasomotion by 50% restriction of blood flow could be due to incorrect brachial occlusion. Incorrect occlusion would yield insufficient restriction for affecting the microcirculatory system in a measurable way. The systolic blood pressure measurements, for determining the total occlusion pressure needed for brachial blood flow restriction of three subjects, showed high values around 140 mmHg and 150 mmHg outside the normal, which is around 120 mmHg for the systolic blood pressure[4]. Since those three subjects were in different age and shape, a suspicion for incorrect values arise. Even if the blood pressure monitor delivered incorrectly high values, the outcome of the restriction period would not have been influenced negatively. This would only lead to a calculated occlusion pressure higher than the one needed to reach the intended restriction, which would just lead to a larger difference between both conditions. It would be more problematic with an occlusion level too low. Furthermore all blood pressure measurements were conducted and verified by a professional anesthesiologist. The measured blood pressure values and occlusion pressure can be seen in table 3 in the appendix. An interesting question to rise, is whether or not any vasomotion has been measured in the recordings. A prior study found mean magnitudes of 3.52 and 4.73 for endothelial, 3.73 for neurogenic and 2.96 myogenic frequency band[14]. Comparing these finding to this study's baseline means of 6.71, 5.05 and 4.55, it is seen that this study found a greater

magnitude in every corresponding band. It is assumed that vasomotion contributes to the measured activity, and the higher magnitude in this study might be induced by remaining artifacts. The mean values that the paired t-test is based on, are extracted from the CWT data in the specific frequency bands. Though the cone of influence (COI), displayed in the scalograms as gray fading, has not been taken into consideration. The areas outside of the COI mark regions of the CWT containing areas of uncertainties, because of the bigger window size needed for the computation of the lower frequency content[14].

The use of the paired t-test was mainly due to the study design, where it is determined if there will be a significant difference in vasomotion, between the baseline and the restriction, within subjects. It was assumed that the data was normal distributed because of a natural variance within the population, why a parametric test was used. But with the small sample it was not possible to determine the actual distribution. In case of non-normally distribution a non-parametric test should be used. In this case a Wilcoxon signed rank test would be the approach for the statistical test. This test does not require a normal distribution in the population and is focusing on the population median value instead of the population mean like the paired t-test[15].

ii. Critique of study design

The small sample size of four subjects applied to the statistical methods are not sufficiently meaningful. With a larger amount of subjects this study would get a more representative result. Originally a larger amount of subjects was planned to be recruited for the experiment. However, the notice of artifacts in the temperature trace lead to the choice of not recruiting more subjects. Instead the focus was put on finding the origin of these artifacts and a way to bypass these. Instead of trying to bypass these artifacts in the data processing, other experiment testing camera operation in more controlled settings could have been carried out. Furthermore the statistics might not have led to any valid results with these artifacts in the temperature trace, even with a greater amount of subjects.

Stabilizing the subject's hand by a vacuum pillow was done with the assumption that the subjects were still, but this does not give sufficient support to inhibit every movements of the subject. A mechanism for better stabilization of the hand should be included. Else image alignment in the data processing to limit the drawbacks of possible movements in the recordings could have been included. Furthermore with the used setup exact same conditions for each subject cannot be granted. For instance the ambient temperature might have had an effect on the recording. It is noticed that subject 1 had a skin temperature of around 38°C compared to the skin temperature of around 26°C of subjects 2 and 3. Both were having cold hands during the baseline recording. Looking at the ambient temperature in the recordings of areas outside of the hand stating a temperature of 25.83 $\pm$0.99 °C, being highest at subject's 1 recording. Other explanations than the room temperature, for the great difference in subject hand temperature should be considered, like mental state of the subjects and activity prior to the experiment. The software settings should be verified and if necessary changed beforehand of the experiment to fit the circumstances. An optimization of the test setting would require a more controlled setup of the experiment and a thermal camera of higher quality preferable of a cooled type.

iii. Limitations in using thermal camera

Due to the corrupted temperature reading the correction method was implemented, which clearly affects parts of the temperature trace in specific ROIs. The pixel drift increases with increasing distance to the center of the thermal image why pixel drift of ROIs located in the outer areas of the thermal image cannot be completely compensated with the implemented correction method[13]. The correction

method shows another weak point in correcting the drift when the hand's overall temperature changed during a recording. The explanation for bot,h is likely that the correction method was based on the assumption that the drift component in every interval is linear[13]. If the drift component is linear, the correction method works fine for linear temperature traces. Though this assumption borders the correction of non-linear temperature traces by enhancing discontinuities. The limitation of correcting temperature traces with an overall temperature change arise the suspicion that the correction method might rule out the micro oscillations in temperature. Besides, the assumption of a linear drift component might be wrong and a correction method that uses another regression method or combines different regression methods might adjust the artifacts in a better way. Another camera might also be preferable to reduce the risks of technical artifacts like these. It should be noticed that in the baseline recording of subject 2, no discontinuities occurred. This subject is the only in which there can be seen a pattern as a decrease in the mean magnitude of all the frequencies bands from the intervention, this is further illustrated on figure 8. If no discontinuities had been present, the general tendency of the mean magnitudes from the data might have looked different, assumable with a decrease in mean magnitude like in subject 2's case.

Furthermore the closer the thermal camera to the observed area, the smaller the area represented by one pixel. Within this study one pixel represents an area with a diameter around 417μm. Capillaries have an average diameter of 8μm[14]. As the interest lies in observing several capillaries within a capillary bed, a ROI should be larger than the diameter of one capillary. But with the use of a too large ROI, it might be that the amount of inverse dilating capillaries is equal and thereby canceling each other out. Due to inverse dilating capillaries there might be no changes over time measurable because the frequency contents are occurring alternating in the different capillaries. In addition, the artifact content in the temperature trace was significantly higher than in the temperature traces detected in previous studies. Comparing the temperature traces, the question arises, if the artifacts overlap or suppress the frequency content of vasomotric activity. Even though temperature changes over time in the skin were detected, it is uncertain, if this temperature traces just represents the general skin temperature or also vasomotric activity.

V. Conclusion

The results of this study indicate that thermal imaging is not sensitive enough for detecting changes in vasomotion during a 50% restriction of blood supply. No statistical significant difference between the two conditions was found, indicated by the p-values in table 2. Despite no findings, this study provides information about key points that should be considered when studying vasomotion with thermal imaging. For instance that the regions of most interest should be placed in the center of the thermal image to reduce drift as much as possible, and the importance of thermal camera specification. Further investigation in this field is needed, to investigate if thermal imaging is a promising technique for detecting changes in vasomotion.

VI. Acknowledgment

The authors would like to thank Lasse Riis Østergaard, Carsten Dahl Mørch and Andrei Ciubotariu for the cooperation and great advice during this study. Furthermore we are Region Hospital Nordjylland thankful for the use of their facilities during the experiment.

References

[1] Ronald V. Maier. Approach to the Patient with Shock. In: Harrison's Principles of medicine 18 (2012). url: http://accessmedicine.mhmedical.com/content.aspx?bookid=331%7B%5C&%7Dsectionid=40727056.

[2] Can Ince. The microcirculation is the motor of sepsis. In: Critical care (London, England) 9 Suppl 4.Suppl 4 (2005), S13-9. issn: 1466-609X. doi: 10.1186/cc3753. url:http://www.ncbi.nlm.nih.gov/pubmed/16168069%7B%5C%%7D5Cn

[3] Tang YL, He Y, Shao HW, Mizeva I. Skin temperature oscillation model for assessing vasomotion of microcirculation. Acta Mechanica Sinica. 2015; 31(1): 132-138.

[4] Martini FH, Nath JL, Bartholomwe EF, Fundamentals of Anatomy and Physiology Ninth Edition, pp. 707-800. isbn-13: 978-0-321-70933-2.

[5] H. Nilsson. Vasomotion: Mechanisms and Physiological Importance. In: Molecular Interventions 3.2 (2003), pp. 79-89. issn: 1534-0384. doi: 10.1124/mi.3.2.79. url: http://molinterv.aspetjournals.org/cgi/doi/10.1124/mi.3.2.79.

[6] Steven S. Segal. Regulation of blood flow in the microcirculation. In: Microcirculation 12.1 (2005), pp. 33-45. issn: 10739688. doi: 10.1080/10739680590895028.

[7] Sagaidachnyi et al. Thermography-based blood flow imaging in human skin of the hands and feet: a spectral filtering approach. In: Physiological Measurement 38.2 (2017), pp. 272-288. issn: 0967-3334. doi: 10.1088/1361-6579/aa4eaf. url: http://www.ncbi.nlm.nih.gov/pubmed/28099162%7B%5C%%7D5Cnhttp://-stacks.

[8] Mary Jo Geyer et al. Using wavelet analysis to characterize the thermoregulatory mechanisms of sacral skin blood flow. In: Journal of rehabilitation research and development 41.6A (2004), pp. 797-806. issn: 0748-7711. doi: 10.1682/JRRD.2003.10.0159.

[9] Sagaidachnyi et al. Determination of the amplitude and phase relationships between oscillations in skin temperature and photoplethysmography-measured blood flow in fingertips. In: Physiological measurement 35.2 (2014), pp. 153-66. issn:1361-6579. doi: 10.1088/0967-3334/35/2/153. url:http://www.ncbi.nlm.nih.gov/pubmed/24399251.

[10] Wei Min Liu et al. Reconstruction of thermographic signals to map perforator vessels in humans. In: Quantitative InfraRed Thermography Journal 9.2 (2012), pp. 123-133. issn: 21167176. doi: 10.1080/17686733.2012.737157.

[11] J. Grant Mouser et al. A tale of three cuffs: the hemodynamics of blood flow restriction. In: European Journal of Applied Physiology 117.7 (2017), pp. 1493-1499. issn: 14396319. doi: 10.1007/s00421-017-3644-7.

[12] Anders Eriksen, Dominik Osinski, and Dag Roar Hjelme. Evaluation of thermal imaging system and thermal radiation detector for real-time condition monitoring of high power frequency converters. In: Advances in Manufacturing 2.1 (2014), pp. 88-94. issn: 21953597. doi: 10.1007/s40436-014-0066-1.

[13] Robert Olbrycht and Boguslaw Wiecek. New approach to thermal drift correction in microbolometer thermal cameras. In: Quantitative InfraRed Thermography Journal 12.2 (2015), pp. 184-195. issn: 21167176. doi: 10.1080/17686733.2015.1055675. url: http://dx.doi.org/10.1080/17686733.2015.1055675.

[14] Wei Min Liu et al. Observing temperature fluctuations in humans using infrared imaging. In: Quant Infrared Thermography Journal 8.1 (2011), pp. 21-36. doi: 10.3166/qirt.8.21-36.

[15] Akeyede Imam, Usman, Mohammed. and Chiawa, Moses Abanyam. On Consistency and Limitation of paired t-test, Sign and Wilcoxon Sign Rank Test (2014), pp. 01-06. e-issn: 2278-5728, p-issn: 2319-765X. doi: 10.9790/5728-10140106.

VII. Appendices

Table 3: *Table of blood pressure written into the experimental protocol.*

Subject number	1. systolic pressure	2. systolic pressure	3. systolic pressure	Mean pressure	30 % of TOP
1	141 mmHg	138 mmHg	137 mmHg	138.6 mmHg	54.08 mmHg
2	102 mmHg	102 mmHg	102 mmHg	102 mmHg	39.78 mmHg
3	155 mmHg	147 mmHg	146 mmHg	149.3 mmHg	58.24 mmHg
4	138 mmHg	145 mmHg	135 mmHg	139.3 mmHg	54.34 mmHg

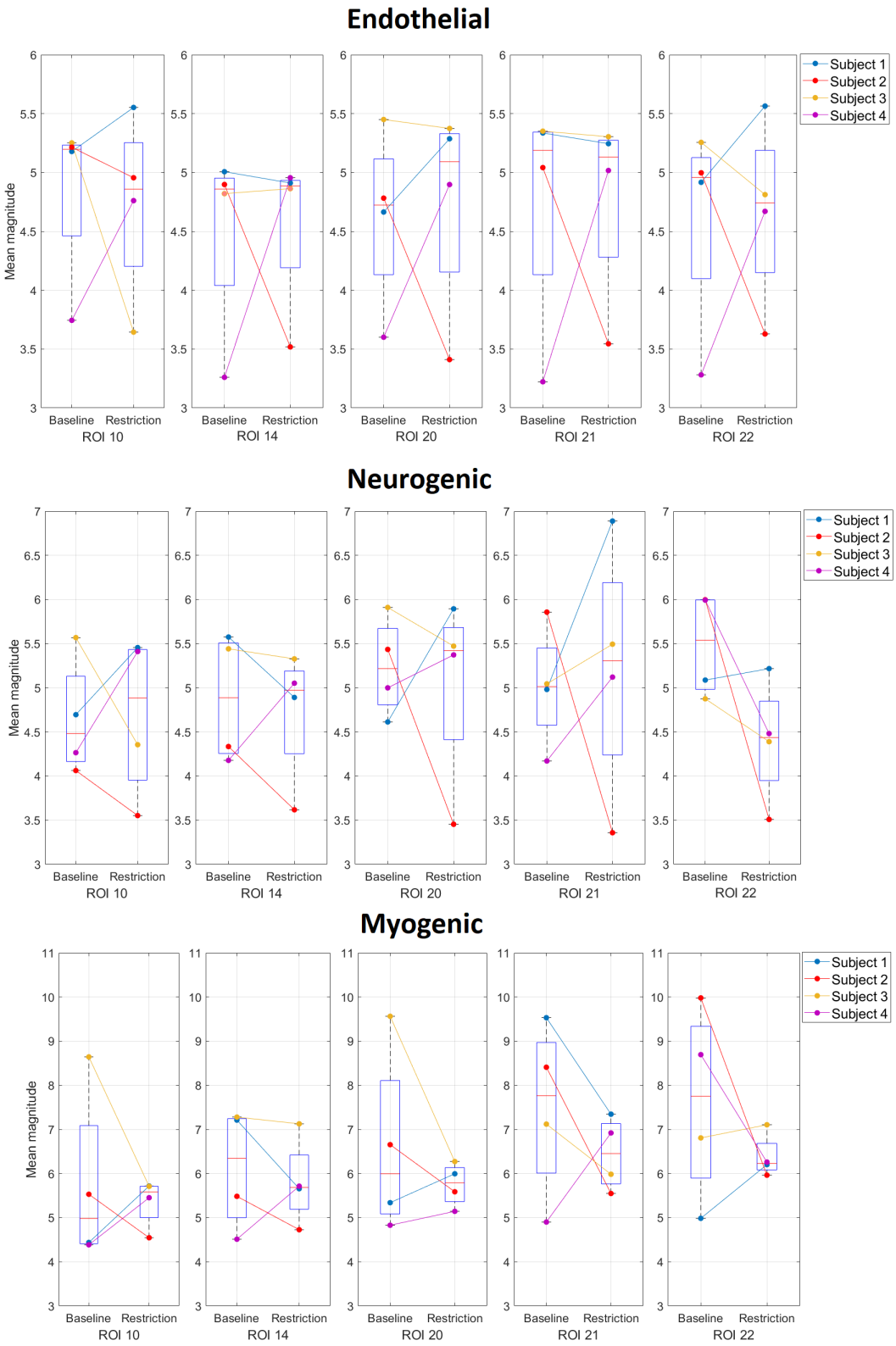

Figure 8: *Box plots showing the mean magnitudes for each subject indicated by color within endothelial, neurogenic and myogenic frequency bands for ROI 10, 14, 20, 21 and 22.*